WILEY-VCH

DOI: 10.1002/ ((please add manuscript number))
Article type: Full Paper

Fast response, highly air-stable, and water-resistant organic photodetectors based on a single crystal Pt complex

Dharmaraj Periyanagounder,[a,#] Tzu-Chiao Wei,[a,#] Ting-You Li,[a,d] Chun-Ho Lin,[a] Théo Piechota Gonçalves,[e] Hui-Chun Fu,[a] Dung-Sheng Tsai,[a] Jr-Jian Ke,[a] Hung-Wei Kuo,[b] Kuo-Wei Huang,[e] Norman Lu,[b,d] Xiaosheng Fang,*[c] and Jr-Hau He*[a,f]*

[a] Computer, Electrical, and Mathematical Sciences and Engineering Division, King Abdullah University of Science & Technology, Thuwal 23955-6900, Saudi Arabia

[b] Institute of Organic and Polymeric Materials, National Taipei University of Technology, Taipei 106, Taiwan, ROC

[c] Department of Materials Science, Fudan University, Shanghai 200433, P. R. China

[d]Department of Molecular Science and Engineering, National Taipei University of Technology, Taipei, Taiwan, ROC

[e] KAUST Catalyst Centre, Physical Science and Engineering Division, King Abdullah University of Science & Technology, Thuwal 23955-6900, Saudi Arabia

[f] Department of Materials Science and Engineering, City University of Hong Kong, Kowloon, HK SAR, China

*jrhauhe@cityu.edu.hk, xshfang@fudan.edu.cn, normanlu@mail.ntut.edu.tw

Keywords: organic photodetector, metal-ligand charge transfer, organic semiconductor, fluorine functionalization, transfer integral

Abstract:

Organic semiconductors demonstrate several advantages over conventional inorganic materials for novel electronic and optoelectronic applications, including molecularly-tunable properties, flexibility, low-cost, and facile device integration. However, before organic semiconductors can be used for the next generation of devices, such as ultrafast photodetectors (PDs), it is necessary to develop new materials that feature both high mobility and ambient stability. Toward this goal, we demonstrate a highly stable PD based on organic single crystal [$PtBr_2$(5,5′-bis($CF_3CH_2OCH_2$)-2,2′-bpy)] (or “Pt complex (1o)”) as the active

semiconductor channel - a material that features a lamellar molecular structure and high-quality, intra-ligand charge transfer. Benefitting from its unique crystal structure and fluorine-containing substituents, the Pt complex (1o) device exhibits a field effect mobility of ~0.45 cm^2/V s without loss of significant performance under ambient conditions even after 40 days without encapsulation, as well as immersion in distilled water for a period of 24 h. Furthermore, the device features a maximum photoresponsivity of 1×10^3A/W, a detectivity of 1.1×10^{12} cm $Hz^{-1/2}$ W^{-1} at 5 V, and a record fast response/recovery time of 80/90 μs, which has never been previously achieved in other organic PDs. Our findings strongly support and promote the use of single crystal Pt complex (1o) in the next generation of organic optoelectronic devices.

1. Introduction

Photodetectors (PDs) are sensors of electromagnetic radiation and are at the core of many technologies applied in chemical and biological analysis, combustion flame monitoring, image sensors, remote controls, optical communications, night vision, and machine version.[1-3] PDs displaying high responsivity and speed are typically made using inorganic semiconductors, leveraging the high mobility and stability of these materials. However, conventional inorganic PDs with low strain tolerance are limited to rigid substrates and gradual electrical changes, in which large mechanical strain can lead to the deterioration of the spectral response or result in device failure.[3] The next-generation of consumer electronics will involve devices that are more flexible and portable. Fortunately, organic semiconductors, which feature molecularly-tunable properties, excellent semiconductivity, and facile and low-temperature processing, have emerged as a new class of revolutionary materials that represent an alternative to commercial inorganic-based PDs. Moreover, organic semiconductors offer several benefits, in that they are lightweight, thin, flexible, semi-transparent, and offer simple device integration and compatibility with plastic substrates and biological systems. Most importantly, they are more eco-friendly compared to inorganic semiconductors.

Despite being an outstanding material for various applications, the stability and electrical properties of organic semiconductor are not yet fully optimized. Generally, organic semiconductors are limited by low carrier mobility and high threshold voltage due to carrier scattering caused by impurities, structural defects, and grain boundaries, which hinder the development and integration of these materials for high performance and low-cost applications.[4] As a result, single crystals of organic semiconductors are the cornerstone of modern organic electronic devices due to their reduced trap density and lack of grain boundaries, thus avoiding the carrier scattering phenomena and greatly improving the device mobility and viability.[5-7]

The use of single crystals would significantly improve the performance of organic PDs, but the real challenge is the stability of these materials, which remain inferior to that of inorganic semiconductors. Devices based on organic single crystals (such as hexacene, pentacene, and tetracene) significantly degrade upon exposure to air and/or moisture, leading to short device lifetimes. [8, 9]. For example, the life-time of a single crystal hexacene transistor without encapsulation is only ~19 days,[8] while pentacene suffers from photo-oxidation and quickly degrades to form transannular endoperoxides when exposed to light and oxygen in a solution medium.[9] Additionally, devices made using n-type organic semiconductors always display poorer stability than p-type devices since electrons in n-type devices are more prone to trapping processes when exposed to water and air due to mismatched energy band alignment.[10] Encapsulating the device with a high barrier material can help preserve the organic semiconductor from environmental effects, however, this can add to the complexity of the device fabrication. Therefore, it remains a challenge to simultaneously achieve the various advantages of organic semiconductors, including their low-cost fabrication, high photosensitivity, fast response speed, long-term stability, and high charge carrier mobility within a single device.

No matter what kind of materials and processing used, the success of organic devices ultimately relies on two factors: mobility and stability under ambient and extreme conditions, which determine the overall device performance. Bearing these in mind, current research efforts have aimed to develop highly stable n-type organic materials that can work under such conditions by engineering the crystal structure.[10] This involves designing and synthesizing functional molecular solid-state structures and intermolecular interactions to achieve high mobility for targeted applications.[11-15] The combination of two approaches appears very promising not only to obtain highly stable organic semiconductors, but also to concurrently improve the mobility. The first approach involves the use of organic semiconductors with a lamellar molecular structure, which benefits charge carrier transport and thus improved mobility.[10] However, such lamellar organic structures have been associated with poor stability under ambient conditions.[16] To overcome this limitation, the second key strategy involves the incorporation of fluorine atoms into the organic molecular structure, which not only promotes air stability but also greatly improves the material's water-repellent properties, making the lamellar organic semiconductor highly stable in ambient conditions without sacrificing its mobility. [10,17-23]

With these attributes in mind, we recently developed [$PtBr_2$(5,5′-bis($CF_3CH_2OCH_2$)-2,2′-bpy)], a linear-chained single crystal organic semiconductor featuring lamellar structures and fluorine-containing segments,[24,25] which we refer to as the "Pt complex (1o)" for simplicity. The crystal structure of the Pt complex (1o) with its unusual structural and photoluminescent properties has been explored previously.[24] However, there has been little study of optoelectronic devices based on this type of poly-fluorinated Pt complex (1o).

In this work, we report the efficient fabrication of PDs based on this single crystalline, poly-fluorinated Pt complex (1o), which renders the device with high field-effect mobility of up to 0.45 cm^2/V s at a threshold voltage as low as 1.12 V. Benefiting from the lamellar molecular structure and incorporation of fluorine groups, the device also exhibits long-term

stability in air and distilled water. Additionally, the device structure exhibits an excellent photoresponsivity of 1000A/W, an ON/OFF ratio of 16, a response/recovery time of 80 μs/90 μs, and polarization sensitivity, thereby demonstrating its stable and fast photoswitching capability. Thus, the present work demonstrates the potential of a new generation of fast, stable, and water-resistant PDs based on polyfluorinated single crystal organic materials with impressive consistency and long-term repeatability.

2. Results and discussion

2.1 Design, fabrication, and preliminary characterization

Figure 1(a) shows the single crystal structure of the polyfluorinated Pt complex (1o) based on X-ray diffraction (XRD) spectroscopy (see experimental section for details). The crystalline Pt complex (1o) has a lamellar molecular structure with a quasi-linear Pt···Pt···Pt chain that is formed by two neighboring Pt metal atoms located at the center of two different dimer-pairs. The Pt-Pt distances were 3.590 Å within the dimer-pair unit and 3.619 Å between the two closest neighboring units (Figure 1(a)). The strong supramolecular interactions of Pt···Pt···Pt among the dimer-pairs leads to the linear-chain-like structure in which the Pt···Pt···Pt angle is up to 168°. In addition, the Pt complex (1o) has bulky fluorine-containing side chains substituted at the 5,5′-positions of the 2,2′-bipyridine ligand. [24]

In order to reveal the energy transition dynamics, we measured the photoluminescence (PL) spectrum of the material with an excitation wavelength of 325 nm at room temperature (Figure 1(b)). The lowest-energy excited state peak observed at ~675 nm can be mainly assigned to the metal-to-ligand charge transfer (MLCT) transition (an electron transition from the metal to ligand molecular orbitals[26]), which is consistent with previous observations based on other Pt(II) complexes. [27-29] The peak at ~400 nm also confirms the π-π* transition from the bipyridyl ligand moiety in the organic crystal. [30] Thus, the crystal structure of the Pt complex (1o) adopts both a 1D linear chained wire and a lamellar molecular structure with 2D π-π stacking, providing a large transfer integral that should result in high mobility.

Figure 1(c) displays a schematic diagram of the fabricated PD device, in which the Pt complex (1o) serves as the active semiconductor material. To the best of our knowledge, this is the first PD demonstrated using aliphatic fluorine-containing side-chains, linear chained single crystals with Pt···Pt···Pt interactions, and an MLCT transition. To validate the feasibility of the Pt complex (1o) for this application, we performed in-depth electronic, optoelectronic, and stability studies, including characterization of the material's (i) temperature-dependent electrical transport, (ii) field-effect mobility and stability, (iii) water repellant properties, (iv) photoresponsivity, (v) photoresponse and recovery time, and (vi) polarization-dependent photodetection.

First, in order to determine the electronic nature of the polyfluorinated single crystal Pt complex (1o), we measured the electrical conductance at different temperatures, as presented in Figure 1(d). We observed a clear trend of increasing conductance with temperature (from 250–300 K), indicating the excellent semiconducting behavior of the Pt complex (1o) crystal. Note that the lamellar molecular structure (which provides a strong electronic coupling for both electrons and holes), MLCT and oxidation states of the metal are the primary factors responsible for the semiconducting behavior, as well as the high conductivity of the fluorinated Pt complex (1o) crystals. Even though this polyfluorinated Pt complex (1o) is a thermally stable crystal, we observed that it undergoes a phase change when the temperature is below 250 K. Therefore, we conducted the temperature-dependent study from 250–300 K to avoid complicating the analysis. The details about the phase change at lower temperatures are currently under investigation and will be published elsewhere. To obtain an in-depth understanding of the characteristics of a single crystal of the Pt complex, we have conducted a theoretical study of the integral transfer calculation.[31] This key parameter, which governs the charge transport in the Pt complex (1o), was obtained for different axes of the crystal, as presented in Figure 2. It clearly reveals that the charge transport in single crystal Pt complex (1o) is direction dependent and the high transfer integral for electrons suggests that the

electron transport is expected to favorably proceed along the direction parallel to the molecular packing (side-to-side dimer). Besides, as the crystal exhibits different electronic coupling along different axes, it is also predicted that the single crystal Pt complex (1o) may behave as ambipolar semiconductor with high electron (hole) conductivity in in-plane molecular (π-π stacking) direction. This also indicates the excellent semiconducting property of the Pt complex (1o) and its electronic properties can be varied by tuning its molecular structure.[25]

2.2 FET characteristics of the single crystal Pt complex (1o)

Figure 3a shows the I_{DS}-V_{DS} characteristics of the Pt complex (1o) PD at different gate voltages in the dark. The charge transport characteristics of the device was measured in in-plane molecular direction (along side-to-side type dimer). The drain current of the device was well controlled and tunable by the gate voltage, exhibiting clear field effect transistor (FET) device operation (as shown in the inset of Figure 3a). The device displayed n-type semiconductor behavior with a mobility (μ) of 0.45 cm^2/V s at a threshold voltage as low as 1.12 V, estimated according to the formula: [32]

$$\mu = \left(\frac{L}{W\ C_g V_{SD}}\right)\left(\frac{dI_{DS}}{dV_G}\right) \qquad (1)$$

in which C_g is the capacitance per unit area of the insulating gate, L is the channel length, W is the channel width, V_G is the gate voltage, and I_{DS} is the source-drain current. The mobility value is higher than that of other quasi-linear-chain complexes, such as [Pt-$(NH_2dmoc)_4$][$PtCl_4$], which features a mobility between 0.01-0.1 $cm^2\ V^{-1}\ s^{-1}$ [33], and the well-known n-type single crystalline $F_{16}CuPc$, which features a relatively low mobility of ~5.32 × $10^{-4}\ cm^2\ V^{-1}\ s^{-1}$. [34]

It has been widely reported that devices based on n-type materials (p-type) display poor (superior) charge transport characteristics due to mismatched (well-matched) band alignment between the work function of Nobel non-oxididant metals and the LUMO (HOMO)

of the n-type (p-type) semiconductor, resulting in low (high) mobility.[10] Despite these facts, we attribute the high electron mobility observed in our device to three reasons. First, employing a lamellar structure with strong supramolecular interactions contributes to the increase of the transfer integral as the molecules are packed in such a way that charge carrier transport is facilitated over a straight line. This provides the shortest route for efficient charge transport within the crystal as the organic molecules are packed along the direction of the current flow, [24] resulting in high mobility. [10,33,35] Furthermore, as presented in Figure 2, our theoretical calculations reveals the larger intermolecular electronic coupling (transfer integral) for electrons (17.7 meV) along side-to-side type dimer, which might validate the observed high electron mobility toward the charge transport direction in the channel. Secondly, the substitution of electron withdrawing element (-F-) into the semiconductor and/or the d_z^2 and d_z^2 orbital interactions of the Pt atoms from the linear Pt···Pt···Pt chain lowers the LUMO level, facilitating barrier free transport toward high mobility. Third, the Pt complex (1o)'s ideal single crystalline structure minimizes charge traps, eliminates grain boundaries, and provides highly stable chemical properties, which allows the material to display its intrinsic material characteristics, including a higher mobility compared to polycrystalline or other organic semiconductors.

2.3 Stability measurements in air and water

As the operation of organic optoelectronic devices strongly depends on their electrical stability over time, it is necessary to examine the stability of the field effect mobility. Therefore, we investigated the time-dependent performance/decay of the Pt complex (1o) PD, as shown in Figure 3b. No obvious degradation was observed over a period of 40 days even without encapsulation under ambient conditions, with an average mobility of ~0.45 cm^2/Vs, indicating the remarkable electrical stability of the Pt complex (1o). The crystal's high stability and low threshold voltage can be ascribed to the absence of charge traps at the interface between the Pt complex (1o) crystal and the gate dielectric, as well as the material's

ideal crystal geometry. Furthermore, this type of fluorinated Pt complex (1o) crystal does not contain any -OH groups to act as charge trapping sites, which can lead to degradation of the device over a long period of operation.[34,36] However, after 90 days, the mobility gradually decreases from 0.45 cm^2/Vs to 0.35 cm^2/Vs (~22%) as a result of mild degradation in the dielectric/channel interface and the crystalline quality of the channel material in atmosphere (Figure 3(b)).[37] Precise control of the surface characteristics of the gate dielectric will greatly improve the interface quality and consequently optimize the FET behavior. In addition, as the molecular tunability of the Pt complex (1o) provides the opportunity for new molecular design, the mobility (or electrical stability) of the device may be further improved by controlling the fluorine substitution. However, excess fluorination may possibly cause adverse effects, such as decreased mobility, indicating that further optimization is needed.

Next, we studied the water tolerance ability of the single crystal Pt complex (1o). For this, we immersed the unpackaged device in distilled water for a period of 24 hours. Remarkably, only a very small decrease (~5.7%) in the field-effect mobility was observed (Figure 3c) due to the gradual removal of ionic impurities by the water.[33] This indicates the extraordinary stability of the Pt complex (1o) PD in water, which we ascribe to the water repelling properties of the incorporation of fluorine-containing groups. Briefly, the high electronegativity of fluorine blocks the polarization of the atom causing hydrophilicity that features the fluorocarbons have low intermolecular attractive forces (*i.e.,* van-der-Waals forces) which strictly prohibit the water to adsorb on its surfaces.[38,39] Furthermore, as compared with traditional organic semiconductor devices (such as those based on hexacene and pentacene), which feature lifetimes as low as ~19-30 days despite high mobilities (~0.4-5 cm^2/V s), [8,40] our device demonstrates a stable performance even under extreme conditions, including more than 90 days in air and 24 h in water. These results indicate that even in extreme conditions, the single crystal poly-fluorinated (1o) can function normally and stably.

Also note that the device test displays comparable performances with only a nominal variation of ±10% over >10 crystal samples.

2.4 Photodetector characteristics of the single crystal Pt complex (1o)

In order to study the ability of the device to respond to light, we measured the dynamic photoresponse under 532 nm illumination (25 mW/cm^2) at atmospheric conditions and different gate voltages. A remarkable increase in the drain current under illumination was observed, as shown in Figure 4(a), indicating that the absorbed photons are effectively converted into photocurrent. Furthermore, the device shows strong field-dependent properties, i.e., the drain current under illumination increases with increasing gate voltage as a result of the increasing number of photo-excited carriers with the applied electric field, yielding typical organic phototransistor characteristics.

To obtain further insight into the practicality of the device, we measured the photoresponsivity (R), which is defined as[41-44]

$$R = \frac{I_{ds,ill} - I_{ds,dark}}{A \times P_{in}} \qquad (2)$$

in which P_{in} is the incident optical power per unit area of the device, $I_{ds,ill}$ and $I_{ds,\,dark}$ are the source-drain currents with and without illumination, respectively, and A is the effective area of the device.[45] The device exhibited a photoresponsivity as high as 1000 A/W at 5 V bias, which is much higher than that of pentacene-based PDs (which is widely regarded as a standard p-type organic semiconducting material),[46,47] F_{16}CuPc (which is the well-known n-type organic semiconductor material) organic phototransistors,[34] and even single crystalline silicon.[48] The high responsivity of the poly-fluorinated Pt complex (1o) PD may be due to its high mobility, efficient carrier collection due to its lack of grain boundaries and/or high defect density, and most importantly its ideal crystal geometry. In other words, the photoresponsivity can be ascribed to the advantages of the well-ordered lamellar molecular structure that permits the transport of photocarriers at high speed.[49,50]

To extend our understanding of the photodetection capability of the Pt complex (1o) semiconductor, we calculated the detectivity (D^*, i.e., the minimum optical signal distinguished above the noise) using equation (3)[42,43,51]

$$D^* = \frac{A^{1/2}R}{\sqrt{2qI_d}} \quad (3)$$

in which I_d is the dark current and q is the electronic charge. We calculated the detectivity of the device to be 1.1×10^{12} cm $Hz^{-1/2}$ W^{-1} at 5 V, demonstrating its practicality for desired applications.[52] It is worth noting that the performance of the Pt complex (1o) can be further enhanced by suppressing the dark current via new crystal engineering, thus potentially offering a way to improve the responsivity and detectivity of the device.[10,53]

2.5 Dynamic photoresponse

Figure 4(b) shows the transient photocurrent of the device as a function of time as we switched the illumination source on and off. At a constant V_{DS} (5 V), the current goes up to a high value (ON state) under 532 nm laser illumination and rapidly goes down to its original value (OFF state) in the dark state. At zero gate bias, the current between the two states yields an on/off switching ratio of 16, which is very fast, repeatable, and reversible. Note that both the photo and dark current are not limited by persistent current effects and the noise level in the ON and OFF state is low and negligible, demonstrating the device's excellent photo-switching and stability.[54, 55]

We also measured the response and recovery times of the Pt complex (1o) PD, which are important figures-of-merit that describe how fast it responds to external illumination. To determine these values, we performed transient photoswitching of the device using an optical chopper to modulate the 532 nm laser. It is apparent that the PD can be reversibly switched between high and low currents as the illumination is chopped at an interval of a few tens of microseconds. As shown in Figure 4(c) and (d), we found that the response time (the time difference between 10% to 90% of the steady-state maximum photocurrent as the light is

switched from OFF to ON) and recovery time (the time difference between 90% and 10% of the maximum photocurrent as the light is switched from ON to OFF) of the Pt complex (1o) PD was 80 μs and 90 μs, respectively. These values are several orders of magnitude faster compared to the response times of other linear-chain-like organic semiconductor devices, such as those based on F_{16}CuPc (~10 ms),[34] crystalline microplates of A-EHDTT (15 s),[56] and other organic semiconductors that feature a very high photoresponse[47,57] (also as shown in Table S1). Furthermore, the photoresponse of the device remains identical over numerous cycles as a result of no obvious charge transfer process that would stimulate carrier recombination. The fast switching speed of our Pt complex (1o) PD is due to the well-proportioned interlaced packing of the molecular structure and the reduction of carrier trapping sites,[35] which renders the material an efficient photosensitive switch. In general, compared with the response time, the recovery time is usually a slow process due to the poor recombination cross-section of trapped carriers.[58] However, the recovery time of our device is nearly identical to the response time, which can be ascribed to the fast recombination cross-section of the photogenerated carriers in the presence of the electric field without any charge transfer effect,[58] resulting in the very fast switching capability of the device.

2.6 Polarization-dependent photoresponse

Next, we explored the polarization sensitivity of the device, an important figure-of-merit for PDs, by varying the polarization of the incident light, as schematically shown in Figure 5a. Figure 5b shows the relationship between the PD responsivity and the relative angle between the incident polarized light along the b axis of the crystal, which is aligned at 0° to the polarizer. The measured photoresponse exhibits a cosine dependence with the angle of the polarization of the incident light, with a maximum to minimum photocurrent ratio of 2, indicating the PD features strong polarization sensitivity. [59,60] In other words, the maximum and minimum photoresponse are attained when the incident light is polarized along the b-axis

and a-axis, respectively, demonstrating the strong anisotropic properties of the single crystal Pt complex (1o). This indicates that more photons are absorbed when they are polarized along the b-axis compared to those polarized along the a-axis. These findings suggest that the Pt complex (1o) crystal can be used for multiphotodetector applications, in which the material can not only sense photons but also measure the polarized state of the incident photons.

Thanks to the unique properties of the Pt complex (1o) crystal, which are made possible by its lamellar molecular structure and fluorine incorporation, we have achieved a breakthrough in organic-material-based PDs in terms of high mobility, photosensitivity, fast response and recovery speeds, long-term stability, polarization sensitivity, and water resistance. However, the important device characteristics (such as mobility, photoresponsivity, and response time) can be further improved by adding functional molecular structures to the crystal.[61] We also note that the quasi-linear Pt···Pt···Pt interaction promotes high hole transfer integral along the π-π stacking direction, as revealed by theoretical calculations.[62] The change in transfer integral along different axis suggests that the single crystal Pt complex may behave as ambipolar semiconductor, thus it requires further study which lays beyond the scope of the present work.

3. Conclusion

In summary, we for the first time demonstrate a highly efficient PD based on a single crystal linear-chain polyfluorinated dibromo-platinum(II) diimine complex. The polyfluorinated Pt complex (1o) crystal features the combined benefits of a lamellar molecular structure and the incorporation of fluorine-containing groups on the side-chains, resulting in very high mobility and stability. The polyfluorinated Pt complex (1o) device demonstrated herein shows a stable mobility (up to 0.45 cm^2/V s at a threshold voltage of 1.12 V) and water-repellant properties (a 22% and 5.7% mobility degradation after 90 days without encapsulation in air and immersion in distilled water for 24 h, respectively). Furthermore, the device features excellent photoresponsivity of 1000 A/W at 5 V bias and an ON/OFF

switching ratio of 16 at zero gate bias, which we attribute to the high gain and low noise of the organic PD's molecular structure. The temporal response of the photocurrent reveals record response and recovery times as fast as ~80 μs and ~90 μs, respectively. In particular, the performance of the device demonstrated here is remarkable compared to other devices featuring organic-semiconductor-based channels. Therefore, the polyfluorinated Pt complex (1o) can serve as a valuable reference for the development of high detectivity, long-term stability, polarization sensitive, and fast photoresponse PDs, as well as for the advancement of future integrated electronic and optoelectronic devices beyond conventional materials and techniques.

4. Experimental Section

4.1 Synthesis and functionalization of the single crystal Pt complex

The preparation of the polyfluorinated Pt complex (1o), [$PtBr_2$(5,5′-bis($CF_3CH_2OCH_2$)-2,2′-bpy)], has been previously reported in ref. 24 and described briefly below. First, equimolar amounts of the fluorinated bipyridine (bpy) ligand, (5,5′-bis($CF_3CH_2OCH_2$)-2,2′-bpy) [24,25,63-65], (197.6 mg, 0.52 mmol) and K_2PtBr_4 (308.3 mg, 0.52 mmol) were added to a round-bottomed flask. Then 3 mL of dried dimethylformamide (DMF) was added as a solvent. After mixing the solution for several minutes, the color changed from red to yellow. Following this, the solution was stirred at 70 °C for 4 h before the solvent and volatiles were removed by distillation. The resultant orange solid was further washed with ether three times to obtain a spectroscopically pure product (i.e., no impurities). In the DMF solution, the resulting complexes were orange in color. By diffusion crystallization, orange red crystals can be obtained. We characterized these crystals as follows:

XRD Characterization. Single crystal X-ray structure analysis of the orange crystals (CCDC 897004) at 250 K: $C_{16}H_{14}Br_2F_6N_2O_2Pt$, M_r = 735.20, P -1, wavelength = 0.71073 Å (Mo K), a = 7.1269(2), b = 9.2336(2), c = 15.9319(5) Å, α = 95.597(1), β = 102.619(1), γ = 94.175(1)°, V = 1013.43(5) Å^3, Z = 2, T = 250.0(1) K, $\rho_{calcd.}$ = 2.409 g cm^{-3}, $2\theta_{max}$ = 54.2°, no.

of reflns = 4368, R = 0.0392, wR2 = 0.0966, GoF = 1.127. The analysis of its X-ray crystallographic data (CCDC 897005) at room temperature is shown in ref. 25.

The XRD patterns were recorded on a Bruker D8 diffractometer with a Bragg–Brentano θ–2θ geometry using a graphite monochromator with Cu K_α radiation. The PL spectra were collected on a confocal PL system (NTEGRA Spectra, NT-MDT) at room temperature. The wavelength of the laser was 325 nm, and the spot size of the laser beam was 0.5 mm.

4.2 Device fabrication and measurements

The single crystal Pt complex (~80 μm^2) was transferred onto a thoroughly cleaned heavily doped Si wafers capped with a 90-nm-thick SiO_2 using mechanical transfer method. A back gated FET geometry was constructed with top Ti/Au (20 nm/80 nm) as Ohmic electrodes deposited by electron beam evaporation and defined by e-beam lithography process. The Ti/Au contacts were patterned such that the Pt complex channel was aligned parallel to the molecular plane direction (side-to-side type dimer), which is the most favorable direction for electron transport in the single crystal Pt complex. Besides using the electron-beam evaporation contacts, we also used contacts painted on the crystal surface with conductive silver ink. Then, a Keithley 4200-SCS semiconductor characterization system was employed to measure the FET and PD characteristics of the device. Temperature-dependent measurements which were carried out by using a Lake Shore TTP4 cryogenic probe station at 5×10^{-6} Torr were conducted in the temperature range from 80 to 300 K. The photocurrent was measured under 532 nm laser illumination (the spot size of the laser beam was ~1 mm) in air at room temperature, and the time-resolved measurements were assisted by a mechanical shutter to switch on/off the laser. The Xray geometry of selected dimers was used to calculate charge transfer parameters. The PW91 functional with all electron (no core) TZP basis set together with scalar relativistic effects was applied for the calculations with ADF software. Post-processing visualization was carried out with the ChemCraft software.

Author Contributions

D. P., T. C. W., T. Y. L., C. H. L., N. L., X. F., and J. H. H. designed the project, prepared samples, conducted experiments, analyzed the data, and wrote the manuscript. H. C. F., J. J. K., D. S. T., and H. W. K. assisted in the device measurements and analyzed the relevant data. T.P.G and K.W.H performed the theoretical studies. N. L., X. F., and J. H. H. supervised the project and directed the research. All authors commented on the paper.

D. P & T. C. W contributed equally to this work.

Acknowledgements

J. H. H. greatly acknowledges the baseline funding from King Abdullah University of Science and Technology (KAUST) and City University of Hong Kong. N. L. thanks the funding from Ministry of Science and Technology in Taiwan (MOST 106-2113-M-001-014-MY3). The authors acknowledge the service of Ibex and Shaheen 2 High Performance Computing Facilities at King Abdullah University of Science and Technology (KAUST).

Received: ((will be filled in by the editorial staff))
Revised: ((will be filled in by the editorial staff))
Published online: ((will be filled in by the editorial staff))

References

[1] M. Itzler, S. Donati, M. S. Unlu, K. Kato, *IEEE Journal of Selected Topics in Quantum Electronics* **2004**, 10, 665.

[2] D.-S. Tsai, W.-C. Lien, D.-H. Lien, K.-M. Chen, M.-L. Tsai, D. G. Senesky, Y.-C. Yu, A. P. Pisano, J.-H. He, *Scientific Reports* **2013**, 3, 2628.

[3] J. Clark, G. Lanzani, *Nature Photonics* **2010**, 4, 438.

[4] L.-N. Nguyen, S. K. Pradhan, C.-N. Yen, M.-C. Lin, C.-H. Chen, C.-S. Wu, K.-S. Chang-Liao, M.-T. Lin, C.-D. Chen, *Applied Physics Letters* **2013**, 103, 183301.

[5] A. L. Briseno, S. C. B. Mannsfeld, M. M. Ling, S. Liu, R. J. Tseng, C. Reese, M. E. Roberts, Y. Yang, F. Wudl, Z. Bao, *Nature* **2006**, 444, 913.

[6] V. C. Sundar, J. Zaumseil, V. Podzorov, E. Menard, R. L. Willett, T. Someya, M. E. Gershenson, J. A. Rogers, *Science* **2004**, 303, 1644.

[7] R. Zeis, T. Siegrist, C. Kloc, *Applied Physics Letters* **2005**, 86, 022103.

[8] M. Watanabe, Y. J. Chang, S.-W. Liu, T.-H. Chao, K. Goto, M. M. Islam, C.-H. Yuan, Y.-T. Tao, T. Shinmyozu, T. J. Chow, *Nature Chemistry* **2012**, 4, 574.

[9] A. Maliakal, K. Raghavachari, H. Katz, E. Chandross, T. Siegrist, *Chemistry of Materials* **2004**, 16, 4980.

[10] C. Wang, H. Dong, W. Hu, Y. Liu, D. Zhu, *Chemical Reviews* **2012**, 112, 2208.

[11] G. R. Desiraju, *Angewandte Chemie* **2007**, 46, 8342.

[12] K.-J. Baeg, M. Binda, D. Natali, M. Caironi, Y.-Y. Noh, *Advanced Materials* **2013**, 25, 4267.

[13] Y. Zhu, J. C. Zhang, J. Zhai, Y. M. Zheng, L. Feng, L. Jiang, *Chem Phys Chem* **2006**, 7, 336.

[14] Y. Zhou, L. Wang, J. Wang, J. Pei, Y. Cao, *Advanced Materials* **2008**, 20, 3745.

[15] T. Hasegawa, J. Takeya, *Science and Technology of Advanced Materials* **2009**, 10, 024314.

[16] T. Lei, Y. Cao, X. Zhou, Y. Peng, J. Bian, J. Pei, *Chemistry of Materials* **2012**, 24, 1762.

[17] R. T. Weitz, K. Amsharov, U. Zschieschang, E. B. Villas, D. K. Goswami, M. Burghard, H. Dosch, M. Jansen, K. Kern, H. Klauk, *Journal of the American Chemical Society* **2008**, 130, 4637.

[18] M.-M. Ling, Z. Bao, P. Erk, *Applied Physics Letters* **2006**, 89, 163516.

[19] J. C. Biffinger, H. W. Kim, S. G. DiMagno, *Chembiochem* **2004**, 5, 622.

[20] J. D. Dunitz, R. Taylor, *Chemistry-A European Journal* **1997**, 3, 89.

[21] S. Uttiya, L. Raimondo, M. Campione, L. Miozzo, A. Yassar, M. Moret, E. Fumagalli, A. Borghesi, A. Sassella, *Synthetic Metals* **2012**, 161, 2603.

[22] H. Klauk, U. Zschieschang, J. Pflaum, M. Halik, *Nature* **2007**, 445, 745.

[23] Z. Bao, *Advanced Materials* **2000**, 12, 227.

[24] N. Lu, L. M. Hight, D. R. McMillin, J.-W. Jhuo, W.-C. Chung, K.-Y. Lin, Y.-S. Wen, L.-K. Liu, *Dalton Transactions* **2014**, 43, 2112.

[25] N. Lu, Y.-M. Ou, T.-Y. Feng, W.-J. Cheng, W.-H. Tu, H.-C. Su, X. Wang, L. Liu, M. D. Hennek, T. S. Sayler, J. S. Thrasher, *Journal of Fluorine Chemistry* **2012**, 137, 54.

[26] J. A. Zuleta, J. M. Bevilacqua, J. M. Rehm, R. Eisenberg, *Inorganic Chemistry* **1992**, 31, 1332.

[27] S.-W. Lai, H.-W. Lam, W. Lu, K.-K. Cheung, C.-M. Che, *Organometallics* **2002**, 21, 226.

[28] W. Lu, M. C. W. Chan, K.-K. Cheung, C.-M. Che, *Organometallics* **2001**, 20, 2477.

[29] J. R. Berenguer, E. Lalinde, J. Torroba, *Inorganic Chemistry* **2007**, 46, 9919.

[30] K.-T. Wang, N. Lu, C.-W. Chu, T.-Y. Feng, C.-C. Kung, W.-H. Tu, Y.-P. Yeh, J. S. Francisco, *Journal of Photochemistry and Photobiology A: Chemistry* **2018**, 358, 100.

[31] A. Solovyeva, M. Pavanello, J. Neugebauer, Describing Long-Range Charge-Separation Processes with Subsystem Density-Functional Theory, *J. Chemical Physics* **2014**, 140, 164103.
[32] W. Hong, G. Jo, S. Kwon, S. Song, T. Lee, *IEEE Transactions on Electron Devices* **2008**, 55, 3020.
[33] W. R. Caseri, H. D. Chanzy, K. Feldman, M. Fontana, P. Smith, T. A. Tervoort, J. G. P. Goossens, E. W. Meijer, A. P. H. J. Schenning, I. P. Dolbnya, M. G. Debije, M. P. de Haas, J. M. Warman, A. M. van de Craats, R. H. Friend, H. Sirringhaus, N. Stutzmann, *Advanced Materials* **2003**, 15, 125.
[34] B. Mukherjee, M. Mukherjee, Y. Choi, S. Pyo, *ACS Applied Materials & Interfaces* **2010**, 2, 1614.
[35] B. Mukherjee, M. Mukherjee, K. Sim, S. Pyo, *Journal of Materials Chemistry* **2011**, 21, 1931.
[36] T. Jung, A. Dodabalapur, R. Wenz, S. Mohapatra, *Applied Physics Letters* **2005**, 87, 182109.
[37] C. S. Kim, S. J. Jo, S. W. Lee, W. J. Kim, H. K. Baik, S. J. Lee, *Advanced Functional Materials* **2007**, 17, 958.
[38] V. H. Dalvi, P. J. Rossky, *Proceedings of the National Academy of Sciences* **2010**, 107, 13603.
[39] D. M. Lemal, *The Journal of Organic Chemistry* **2004**, 69, 1.
[40] X. Yu, J. Yu, W. Huang, L. Zhang, H. Zeng, *AIP Advances* **2012**, 2, 022113.
[41] S.-F. Leung, K.-T. Ho, P.-K. Kung, V. K. S. Hsiao, H. N. Alshareef, Z. L. Wang, J.-H. He, *Advanced Materials* **2018**, 30, 1704611.
[42] C.-H. Lin, B. Cheng, T.-Y. Li, J. R. D. Retamal, T.-C. Wei, H.-C. Fu, X. Fang, J.-H. He, *ACS Nano* **2019**, 13, 1168.
[43] A.M. AlAmri, S.-F.Leung, M. Vaseem, A. Shamim, J.-H.He, *IEEE Transactions on Electron Devices* **2019**, 66, 2657.
[44] W. Yang, J. Chen, Y.Zhang, Y. Zhang, J.-H. He, and X. Fang, *Advanced Functional Materials*, *2019*, 1808182
[45] H. Dong, H. Li, E. Wang, H. Nakashima, K. Torimitsu, W. Hu, *The Journal of Physical Chemistry C* **2008**, 112, 19690.
[46] D. Yang, L. Zhang, H. Wang, Y. Wang, Z. Li, T. Song, C. Fu, S. Yang, B. Zou, *IEEE Photonics Technology Letters* **2015**, 27, 233.
[47] J. Park, J.-H. Seo, S.-W. Yeom, C. Yao, V. W. Yang, Z. Cai, Y. M. Jhon, B.-K. Ju, *Advanced Optical Materials* **2018**, 6, 1701140.
[48] N. M. Johnson, A. Chiang, *Applied Physics Letters* **1984**, 45, 1102.
[49] H.-P.Wang, D.Periyanagounder, A.-C.Li, J.-H.He, *IEEE Access* **2019**, 7, 19395-19400.
[50] A. Alarawi, V. Ramalingam, H.-C. Fu, P. Varadhan, R. Yang, J.-H. He, *Optics Express*, **2019**, 27, A352-A363
[51] C.-H. Lin, H.-C. Fu, D.-H. Lien, C.-Y. Hsu, J.-H. He, *Nano Energy* **2018**, 51, 294.
[52] C.-H. Lin, H.-C. Fu, B. Cheng, M.-L. Tsai, W. Luo, L. Zhou, S.-H. Jang, L. Hu, J.-H. He, *npj 2D Materials and Applications* **2018**, 2, 23.
[53] M. Ramuz, L. Bürgi, C. Winnewisser, P. Seitz, *Organic Electronics* **2008**, 9, 369.
[54] J.R.D. Retamal, C.-H.Ho, K.-T. Tsai, J.-J.Ke, J.-H. He, *IEEE Transactions On Electron Devices*, **2019**, 66, 938.
[55] V.-Q.Le, T.-H.Do, J.R.D. Retamal, P.-W.Shao, Y.-H.Lai, W.-W.Wu, J.-H.He, Y.-L.Chueh, Y.-H.Chu, *Nano Energy* **2019**, 56, 322-329
[56] K. H. Kim, S. Y. Bae, Y. S. Kim, J. A. Hur, M. H. Hoang, T. W. Lee, M. J. Cho, Y. Kim, M. Kim, J.-I. Jin, S.-J. Kim, K. Lee, S. J. Lee, D. H. Choi, *Advanced Materials* **2011**, 23, 3095.
[57] X. Liu, E. K. Lee, D. Y. Kim, H. Yu, J. H. Oh, *ACS Applied Materials & Interfaces*

2016, 8, 7291.

[58] D. Periyanagounder, P. Gnanasekar, P. Varadhan, J.-H. He, J. Kulandaivel, *Journal of Materials Chemistry C* **2018**, 6, 9545.

[59] F. Chu, M. Chen, Y. Wang, Y. Xie, B. Liu, Y. Yang, X. An, Y. Zhang, *Journal of Materials Chemistry C* **2018**, 6, 2509.

[60] J. D. Yao, J. M. Shao, S. W. Li, D. H. Bao, G. W. Yang, *Scientific Reports* **2015**, 5, 14184.

[61] C. Wang, H. Dong, H. Li, H. Zhao, Q. Meng, W. Hu, *Crystal Growth & Design* **2010**, 10, 4155

[62] S. Zhao, F. Yu, G. Yang, H. Zhang, Z. Su, Y. Wang, *Dalton Transactions* **2012**, 41, 7272.

[63] N. Lu, W.-H. Tu, W.-H. Chang, Z.-W. Wu, H.-C. Su, *Acta Crystallogr Sect E Struct Rep Online* **2011**, 67, o355.

[64] T. T. Chang, S. V. More, N. Lu, J.-W. Jhuo, Y.-C. Chen, S.-C. Jao, W.-S. Li, *Bioorg Med Chem* **2011**, 19, 4887.

[65] N. Lu, W.-H. Tu, Y.-S. Wen, L.-K. Liu, C.-Y. Chou, J.-C. Jiang, *Crystal Engineering Communication* **2010**, 12, 538.

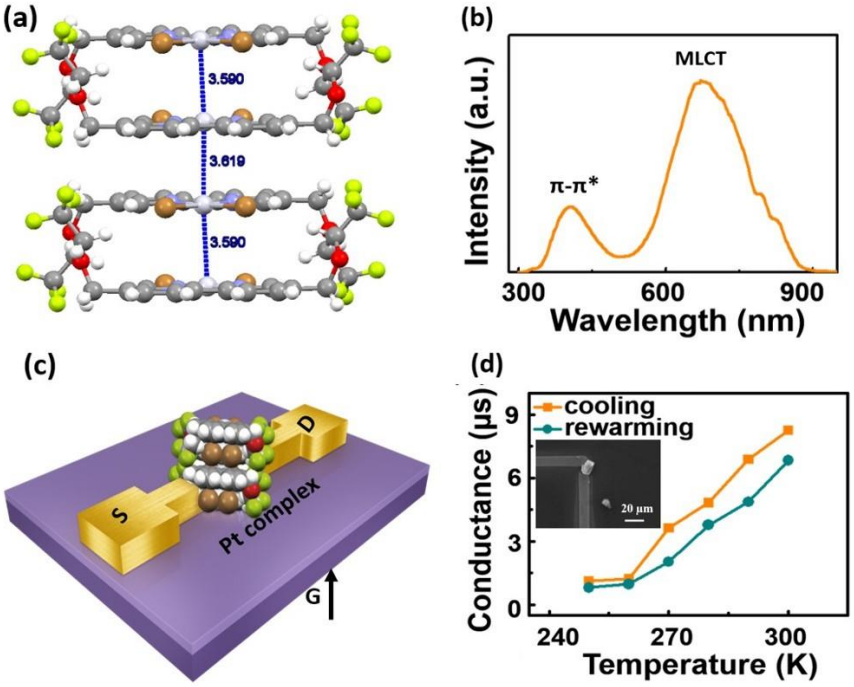

Figure 1. Preliminary characterization of the Pt complex (1o) crystals. A) Two units of stacked dimer-pairs of the Pt complex (1o) crystal. The Pt-Pt distances were 3.590 Å within the dimer-pair unit and 3.619 Å between the two closest neighboring units. [Note: C, H, O, N, F, Br and Pt are in grey, write, red, blue, yellow, brown and silver color, respectively]. **B)** Photoluminescence spectrum of the Pt complex (1o) with an excitation wavelength of 325 nm at room temperature. **C)** Illustration of the structure of the Pt complex (1o) device. **D)** Temperature-dependent conductivity of the Pt complex (1o). Inset shows the SEM image of the fabricate Pt complex (1o) device.

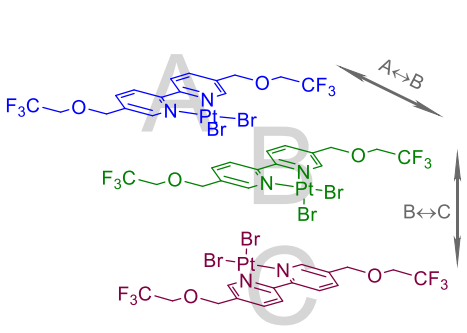

Type of interaction (dimer)	Transfer integral, (10^{-3}eV) Electrons	Holes
Parallel to the molecular plane (A↔B)	17.7	3.0
Perpendicular to the molecular plane (B↔C)	19.7	65.0
Interaction (B↔D)	0.6	0.0

Figure 2. Integral transfer theoretical analysis. X-ray geometry of selected dimers was used to calculate charge transfer parameters and the calculations were conducted with ADF software at PW91/TZP including scalar relativistic effects. The calculation has been carried out for three different molecular packing directions.

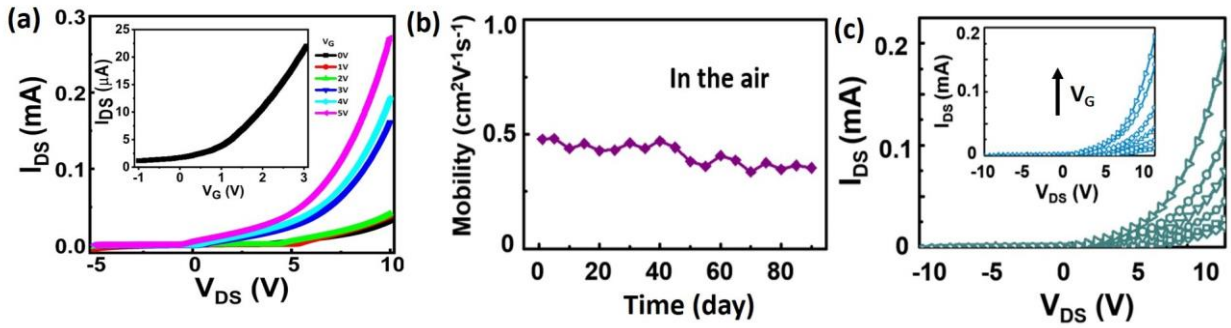

Figure 3. Electron transport and stability characteristics of the Pt complex (1o) single crystal. A) I_{DS}-V_{DS} characteristics of the Pt complex (1o) PD at different gate voltages in the dark (the inset shows the V_G-I_{DS} characteristics of the Pt complex (1o) FET device). **B)** Time-dependent mobility of the Pt complex (1o) under ambient conditions. **C)** I_{DS}-V_{DS} characteristics of the Pt complex (1o) PD and (inset) characteristics of the same device, but stored for 24 h in distilled water.

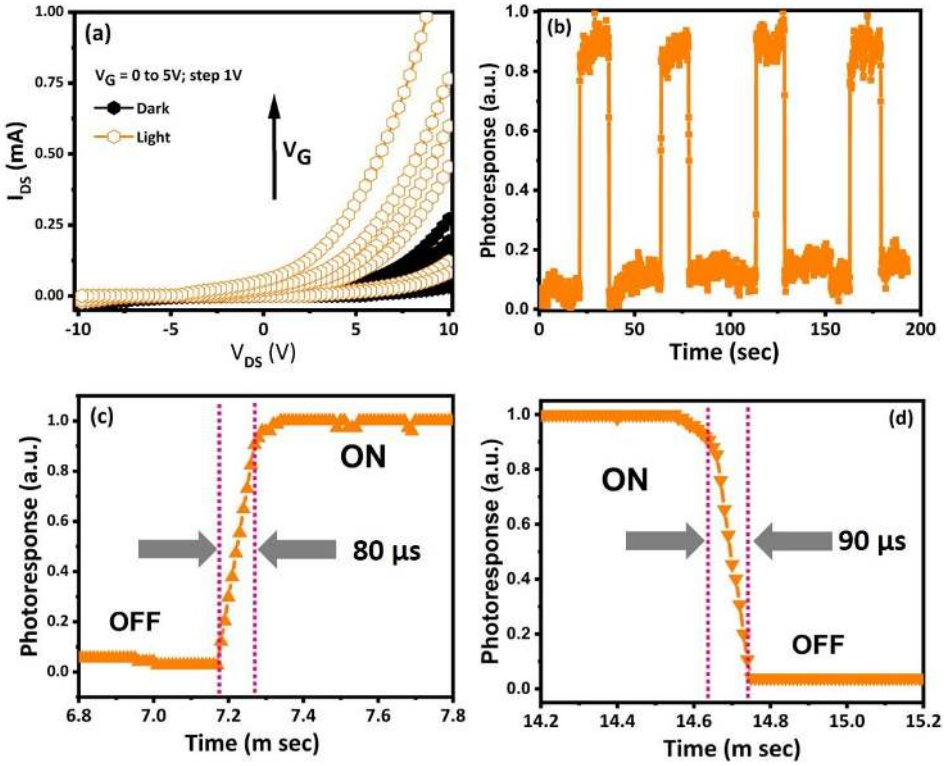

Figure 4. Dynamic photoresponse measurements. A) *I-V* curves of the Pt complex (1o) PD (in ambient air) measured in the dark (closed circles) and under 532 nm illumination with an intensity of 25 mW/cm^2 (open circles). **B)** The photocurrent as a function of time in the dark and under 532 nm illumination (25 mW/cm^2). The high-resolution **C)** response and **D)** recovery times of the Pt complex (1o) PD measured at V_{DS} = 5 V and under 532 nm illumination (25 mW/cm^2).

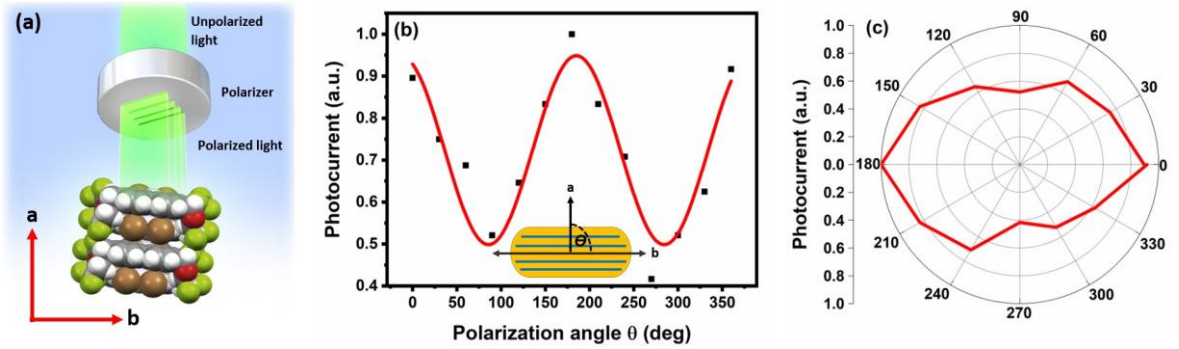

Figure 5. Polarization-dependent photoresponse. A) A schematic representation of the polarization dependent photoresponse measurement. Polarization dependent photoresponse of the Pt complex (1o) in **(B)** Cartezian coordinate and **(C)** Polar coordinate.

In this work, we demonstrate a highly stable PD based on organic single crystal [$PtBr_2$(5,5′-bis($CF_3CH_2OCH_2$)-2,2′-bpy)] (or "Pt complex (1o)") as the active semiconductor channel and/or photo absorption layer for high-performance organic device applications. The Pt complex (1o) device displays a stable mobility (up to 0.45 cm^2/V s at a very low threshold voltage of 1.12 V), highly stable along with a remarkable photoresponsivity of 1000A/W, a record fast response/fall time of 80/90 μs, as well as excellent polarization sensitivity – demonstrating the highest combined efficiency and stability reported for an organic semiconductor.

Keyword: Pt complex, organic photodetector, metal-ligand charge transfer, single crystal organic semiconductor, fluorine functionalization

Dharmaraj Periyanagounder,[a,#] Tzu-Chiao Wei,[a,#] Ting-You Li,[a,d] Chun-Ho Lin,[a] Théo Piechota Gonçalves,[e] Hui-Chun Fu,[a] Dung-Sheng Tsai,[a] Jr-Jian Ke,[a] Hung-Wei Kuo,[b] Kuo- Wei Huang,[e] Norman Lu,[b,d] Xiaosheng Fang,*[c] and Jr-Hau He*[a,f]*

Fast response, highly air-stable, and water-resistant organic photodetectors based on a single crystal Pt complex